Myosin X

17

Hiroshi Tokuo

Abstract

Myosin X (Myo10), an actin-based molecular motor, induces filopodia formation and controls cell migration in vitro. In the 25 years since Myo10 was first identified, it has been implicated in several different functions in different cell types including phagocytosis in macrophages, axon outgrowth in neurons, cell-cell adhesion in epithelial and endothelial cells, podosome formation in osteoclasts, spindle-pole positioning in meiosis and mitosis of cultured cells, migration of melanocytes and cranial neural crest cells, and invadopodia formation in cancer cells. Recently, the availability of Myo10-knockout (Myo10KO) mice has allowed for tremendous progress toward understanding the biological function of Myo10 *in vivo*.

In this chapter, I address the structure of the Myo10 gene; the molecular structure of Myo10 protein with its multiple domains, e.g., PH, MyTH4, and FERM domains; the regulation of actin structures induced in cells by Myo10; the expression and function of Myo10 *in vitro* and *in vivo*; and the role of Myo10 in cancer. Previous reviews on Myo10 include Divito MM, Cheney RE, (Myosins: a super-

family of molecular motors chapter 14 MYOSIN X. In: Proteins and cell regulation, vol 7. Springer, Dordrecht, 2008) and Kerber ML, Cheney RE (J Cell Sci 124:3733–3741).

17.1 Introduction

Myo10 was first identified in 1994 in the sensory epithelia of the inner ear of bullfrogs using a PCR screen with primers based on regions of high amino acid homology among motor domains of myosins known at that time (Solc et al. 1994). By 2000 the full-length cDNA sequences of mouse, human, and cow Myo10 had been determined along with the first information regarding its molecular structure, its wide expression in tissues, and its localization in dynamic actin-rich regions of the cell including membrane ruffles, lamellipodia, and the tips of filopodia (Berg et al. 2000; Yonezawa et al. 2000). The following year, an expressed and purified Myo10 construct representing the head domain and coiled-coil domain of Myo10 was shown to bind to actin filaments

H. Tokuo (✉)
Department of Physiology & Biophysics, Boston University School of Medicine, Boston, MA, USA
e-mail: tokuo@bu.edu

and to hydrolyze ATP, the first demonstration of Myo10's motor activity (Homma et al. 2001). In 2002, expression of exogenous full-length Myo10 was shown to exhibit both forward and rearward movements within filopodia of HeLa cells and to increase both the number and the average length of the filopodia in COS-7 cells (Berg and Cheney 2002). Subsequent studies focused on revealing the identification of its binding partners including phospholipids (Umeki et al. 2011), Mena/VASP (Mammalian enabled/vasodilator-stimulated phosphoprotein) (Tokuo and Ikebe 2004), microtubules (Weber et al.

2004) and integrins (Zhang et al. 2004) in order to gain insight into its cellular functions.

17.2 Gene Structure of Myo10

The class X myosin gene (*MYO10*) is found exclusively in vertebrates and gives rise to the alternatively-spliced proteins full-length Myo10 and headless Myo10 (Sousa et al. 2006). Figure 17.1a shows the genomic structure of mouse *Myo10* and the Myo10KO mouse *Myo10^tm2(KOMP)Wtsi*, which will be discussed in
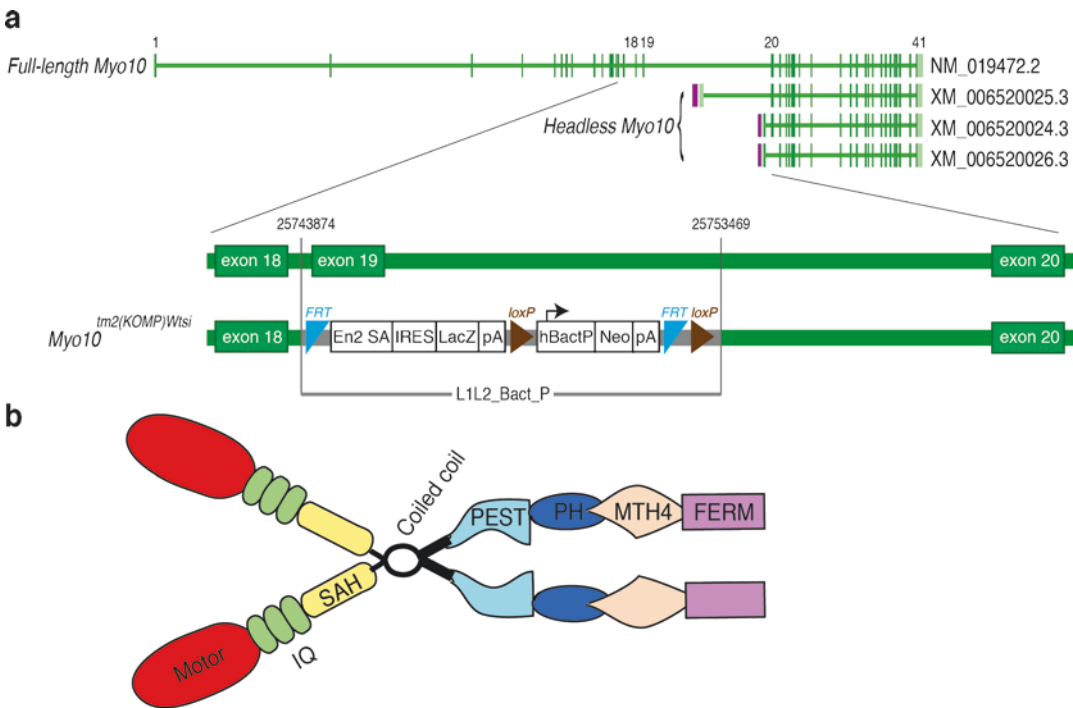
Fig. 17.1 Genomic structure and protein expression of Myo10. (**a**) Allele structure of mouse *full-length Myo10* and three variants formed by alternative splicing referred to as "*headless Myo10*" (top) with magnification of the lesion from exon 18–20. Vertical lines on the schematic gene represent exons, and purple lines represent first exons specific for *headless Myo10*. Below is the genomic structure of *Myo10^tm2(KOMP)Wtsi* in Myo10KO mice in which

the *lacZ* and *neomycin (neo)* expression cassette was inserted between exon 18 and exon 20 (Genome Build GRCm38) resulting in the removal of functionally critical exon 19 and a portion of intron 19 (Tokuo et al. 2018). (**b**) Schematic diagram of a dimerized Myo10 molecule showing its N-terminal motor domain, followed by a neck domain with IQ region, SAH domain, and coiled coil, and tail domain with PEST, PH, MTH4 and FERM domains

Sect. 17.5.1. This Myo10KO strategy is useful in identifying and confirming the expression of splice variants because it deletes full-length, but not headless, Myo10. We detected headless and full-length Myo10 in immunoblots of brain lysates from control mice, but only headless Myo10 in brain lysates from Myo10KO mice, evidence that the *Myo10^{tm2(KOMP)Wtsi}* allele knocks out full-length, but not headless, Myo10.

## 17.3 Structural, Biochemical and Biomechanical Properties of Myo10

The ~237-kDa Myo10 heavy chain consists of a head, neck, and tail domain (Berg et al. 2000). The Myo10 head, or motor, domain has a nucleotide-binding site and an actin-binding site and is responsible for its actin-activated ATPase activity. The neck, or IQ domain, binds three molecules of calmodulin or calmodulin-like protein (Rogers and Strehler 2001; Caride et al. 2010) and consists of a single α-helix (SAH) region (Knight et al. 2005) followed by a coiled-coil region involved in dimerization (Lu et al. 2012). A carboxy-terminal (C-terminal) tail domain, which is primarily involved in cargo binding, consists of four parts: three PEST sequences, which are rich in the amino acids proline, glutamate, serine, and threonine and confer sensitivity to certain proteases, three pleckstrin homology (PH) domains, a Myosin Tail Homology 4 (MyTH4) domain, and a band 4.1, Ezrin, Radixin, Merlin (FERM) domain (Berg et al. 2000) (Fig. 17.1b).

Myo10 exists as both a monomer and a dimer in the cytoplasm. The coiled-coil region following the SAH domain is involved in dimerization and was shown by nuclear magnetic resonance (NMR) spectroscopy to adopt an anti-parallel conformation (Lu et al. 2012). This finding led to the prediction that each of the two heads of dimeric Myo10 could bind to two parallel actin filaments and thus support the movement of Myo10 along actin bundles as well as single filaments (Lu et al. 2012). Previously, a forced dimer of Myo10 heavy meromyosin (HMM) consisting

of the motor, neck, coiled-cold and leucine zipper had been shown to move processively on actin filaments bundled with fascin (Nagy et al. 2008), although in another report using a different forced Myo10 HMM dimer, no selectivity for bundles was observed (Sun et al. 2010). Subsequently, full-length Myo10 molecules (anti-parallel dimers) labeled at the N-terminus with the GFP derivative mWasabi were shown to take 36-nm steps in the forward direction on single actin filaments and steps as large as 52–57nm along fascin-actin bundles (Ropars et al. 2016). The SAH domain and following α-helical domain form a long α-helix that lengthens the Myo10 lever arm and contributes to its ability to take particularly large steps (Ropars et al. 2016). Importantly, Myo10 moves along fascin-actin bundles at a rate nearly twice the rate of on a single actin filament due to an ~two-fold increase in the rate of transition between Pi and ADP release (Ropars et al. 2016).

17.3.1 Monomer-to-Dimer Transition of Myo10 Supports Filopodia Formation

Strikingly, in live-cell imaging studies Myo10 exhibits both forward and rearward movements within filopodia (Berg and Cheney 2002). The speed of the forward movement as determined by total internal reflection fluorescence (TIRF) microscopy is ~600 nm/s in living cells (Kerber et al. 2009), very close to that reported in one recent study tracking full-length Myo10 on fascin bundles (Ropars et al. 2016) and somewhat larger that the 340–780 nm/s reported for movement of a forced dimer of Myo10 heavy meromyosin consisting of the motor, neck, coiled-coil and leucine zipper on artificial actin bundles (Nagy et al. 2008). The rearward movement of Myo10 in filopodia is slow at 10–20 nm/s (Berg and Cheney 2002) and closely matches the rate of the retrograde flow of actin in filopodia. Importantly, only dimerized Myo10 exhibits intrafilopodial motility, suggesting that dimerization of Myo10 is necessary for its proper movement in cells. Moreover, the dimers must form
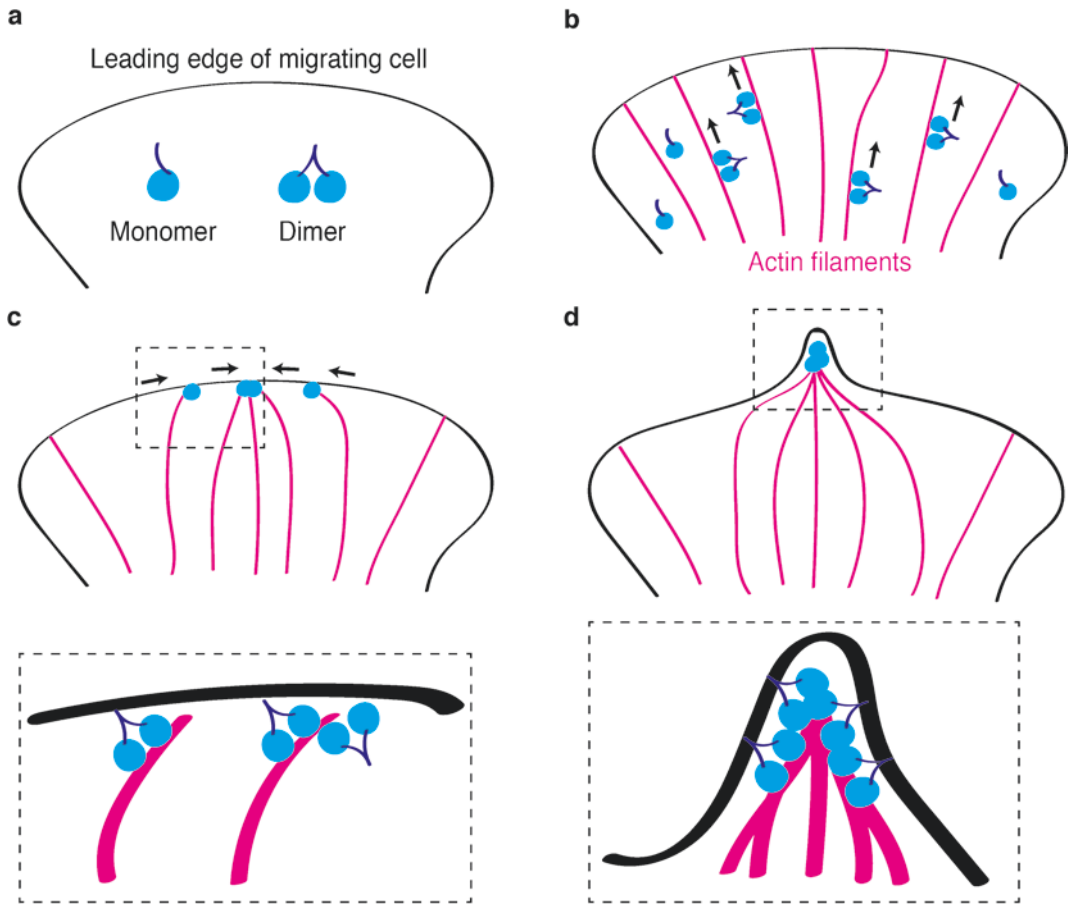
Fig. 17.2 Model of filopodia initiation by dimerization of Myo10. (**a**) Myo10 is present in the cytosol as both a monomer and a dimer. (**b**) Once Myo10 dimerizes to form a two-headed structure, it moves to the tips of the actin filaments. (**c**) The tips of actin filaments move laterally along the leading edge powered by Myo10. (**d**) The lateral drift induces a convergence of the barbed ends of the actin filaments, thereby inducing the formation of microspikes, which develop further into full-length filopodia by actin assembly (Tokuo et al. 2007)

through an antiparallel coiled-coil dimerization or else localization at the tips of filopodia and filopodia induction are compromised (Lu et al. 2012).

Using a dimer-inducing technique we found that when expressed in cells, dimerized tail-less Myo10 induces short unstable filopodia, or microspikes, which may be an initial step in filopodia formation, evidence that the monomer-to-dimer transition of Myo10 induces filopodia in cultured cells (Tokuo et al. 2007). From these results, we advocate a model in which Myo10 exists as both a monomer and a dimer in cells. Although monomeric Myo10 does not localize at the leading edge of migrating cells, after dimerization, Myo10 moves toward the tips of actin filaments at the leading edge, presumably by walking toward the barbed ends of actin filaments (Fig. 17.2). The tips of actin filaments move laterally along the leading edge supported by the mechanical activity of Myo10. Finally, clustering of Myo10 causes convergence of actin filaments into parallel bundles to form the base of the filopodia. This convergence of actin filaments into bundles is likely supported by the structure and flexibility of the Myo10 lever arm, which may facilitate parallel actin filaments being brought together (Ropars et al. 2016).

17.3.2 PH Domains

Pleckstrin Homology (PH) domains are regions of ~120 amino acids with sequence similarity to two regions in pleckstrin (Haslam et al. 1993; Shaw 1993; Mayer et al. 1993), a major substrate of protein kinase C in platelets. This domain, the 11th most common domain in the human proteome, was first recognized for its ability to bind phosphoinositides with high affinity and specificity, although it is now understood that not all PH domains share this property.

Myo10 contains three PH domains. The first PH domain (PH1) is split by the insertion of a second PH domain (PH2). The amino acid sequences of PH1 and PH2 are most similar to that of the PH domain in protein kinase B homologs from *Dictyostelium*, but the sequence of the C-terminal half of the third PH domain (PH3) diverges from that of other PH domains (Berg et al. 2000). PH2 and PH3 contain several residues also found in other proteins that bind phosphatidylinositol lipids phosphorylated by phosphatidylinositol-3-kinase (PI3K) (Rameh et al. 1997; Isakoff et al. 1998).

In a lipid pull-down assay using purified PH domains of Myo10, PH2, but not PH1 or PH3, specifically bound to phosphatidylinositol (3,4,5)-triphosphate (PIP3). Deletion of PH2 or point mutations in PH2 (Lys 1215 to Ala and Lys 1216 to Ala) in full-length Myo10 results in significantly less Myo10 at the tips of filopodia and fewer filopodia (Plantard et al. 2010). These results suggest that PIP3 binding to the PH2 domain of Myo10 is involved in Myo10 trafficking and regulation of filopodia formation. PIP3 binding to the PH domain of Myo10 is also essential for axon development (Yu et al. 2012).

The Arg at position 1231 in Myo10, which is within PH2, corresponds to a conserved residue in the β2 strand of PH domain-containing proteins such as GTPase-activating protein (Gap1) and Bruton's tyrosine kinese (Btk), which is critical for binding to lipid products of PI3K (Salim et al. 1996; Fukuda and Mikoshiba 1996). Insight into the importance of Arg 1231 in Myo10 comes from studies examining phagocytosis in macrophages. Expression of Myo10 tail in macro-phages inhibits phagocytosis by a dominant-negative effect; however, expression of Myo10 tail in which Arg 1231 was mutated to Cys (Myo10 tail[R1231C]) did not change phagocytosis indicating that Arg 1231 is required for the inhibition of phagocytosis by the Myo10 tail (Cox et al. 2002).

17.3.3 MyTH4 and FERM Domains

The myosin tail homology 4 (MyTH4) domain was first named to distinguish it from tail homology domains 1–3 in myosins-I (Hammer 1994). In addition to Myo10, MyTH4 was identified in vertebrate Myo7 (Chen et al. 1996) and Myo15 (Wang et al. 1998). The name of the FERM domain (F for 4.1 protein, E for ezrin, R for radixin, and M for moesin) reflects the initial identification of this domain in a family of peripheral membrane proteins that functions as membrane-cytoskeleton linkers (Chishti et al. 1998). Dozens of FERM domains are encoded by multiple genes in the human genome (Frame et al. 2010). In the myosin superfamily, only Myo7, Myo10, and Myo15 include this domain in the C-terminal tail; these myosins constitute the MyTH4-FERM subfamily of unconventional myosins. The FERM domain consists of three lobes, and lobes F2 and F3 in the FERM domain of Myo10 are required for interaction and relocalization of beta-integrins (Zhang et al. 2004).

MyTH4 and FERM always appear in tandem in Myo7, Myo10, and Myo15. The MyTH4-FERM myosins have conserved physiological functions with all involved in forming actin-rich membrane protrusions: Myo7 in microvilli, Myo10 in filopodia, and Myo15 in stereocilia. Both the FERM domain and the MyTH4 domain are required for the cellular functions of Myo10: deletion of either domain decreases the ability of Myo10 to form filopodia (Bohil et al. 2006; Tokuo et al. 2007; Watanabe et al. 2010).

Myo10 is speculated to exist primarily as a folded monomer in the cytoplasm with its head bound to the PH and FERM domains in the tail; however, association with PIP3 results in its unfolding and dimerization to promote its activ-

ity as a processive motor able to transport cargo (Umeki et al. 2011). This interaction also recruits Myo10 to the cell membrane of the leading edge for filopodia formation (Plantard et al. 2010).

The MyTH4-FERM tandem of Myo10 binds to microtubules, but the individual domains do not (Weber et al. 2004), and binding of Myo10 to deleted in colorectal cancer (DCC) or neogenin also requires a covalent connection between MyTH4 and FERM domains (Zhu et al. 2007). By crystal structure analysis, the MyTH4 and FERM domains interact with each other and form an integral structural supramodule (Wei et al. 2011).

The interaction of Myo10 with microtubules was first identified in 2004 (Weber et al. 2004) as an important factor for nuclear anchoring, spindle assembly, and spindle-F-actin association during meiosis in *Xenopus laevis*. These observations were also confirmed in mitosis of mammalian cells (Toyoshima and Nishida 2007), and the interaction of Myo10 with adducin-1 was found to be essential for mitotic spindle assembly (Chan et al. 2014). Studies of X-ray structures identified specific residues (Lys1645 and Lys1650) within the MyTH4 domain that are essential for direct binding to the acidic C-terminal tail of tubulin (Hirano et al. 2011; Wei et al. 2011; Wu et al. 2011). A double-point mutation in MyTH4 (Lys1645 to Asp and Lys1650 to Asp) in full-length Myo10, which specifically disrupts microtubule binding without altering the interaction of Myo10 with the FERM domain-binding cargo (Hirano et al. 2011), could not rescue the spindle orientation defect resulting from Myo10 knockdown (kd) (Kwon et al. 2015). These results suggest that direct binding of Myo10 to microtubules controls the proper positioning of centrosomes toward retraction fibers and subcortical actin.

17.4 Regulation of Actin Structures by Myo10

17.4.1 Filopodia

Myo10, which specifically localizes to the tips of filopodia, was first identified as an inducer of filopodia (Berg et al. 2000). Filopodia are actin-rich, finger-like protrusions found at the leading edge of cells and believed to modulate numerous cellular processes including cell migration, wound healing closure, adhesion to the extracellular matrix and other substrates, guidance towards chemoattractants and other guidance cues, neuronal growth-cone path finding, and embryonic development in many organs (Mattila and Lappalainen 2008).

Many studies have reported that Myo10 promotes filopodia formation by delivering specific cargos to the cell periphery, e.g., Mena and VASP, which bind to the tail domain of Myo10 (Tokuo and Ikebe 2004; Lin et al. 2013). Myo10-mediated delivery of VASP to filopodial tips would support filopodia elongation as VASP competes with capping protein at the plus end of actin filaments and induces clustering of actin filaments (Applewhite et al. 2007). Myo10 transports integrins to the tips of filopodia for supporting cell attachment to the extracellular matrix (ECM) and promoting filopodia extension (Zhang et al. 2004). In neurites, full-length Myo10 interacts with the netrin receptor DCC to enhance the formation of filopodia, whereas headless Myo10 interacts preferentially with the DCC-related protein neogenin, which could inhibit filopodia formation induced by DCC and Myo10 signaling and axon growth (Zhu et al. 2007). In endothelial cells, Myo10 mediates the transport of VE-cadherin to cell edges and filopodia to support the formation of cell-cell junctions (Almagro et al. 2010).

17.4.2 Podosomes and Invadopodia

In addition to filopodia formation, Myo10 mediates the formation of other actin-based structures such as the adhesive structures podosomes and invadopodia (Schoumacher et al. 2010). Podosomes are found on the ventral side of a variety of cells including osteoclasts, macrophages, and endothelial cells. Myo10 localizes in the podosomal ring of osteoclasts between actin and microtubules and participates in osteoclast attachment and podosome

positioning by directly linking actin to microtubules.

Invasive cancer cells display membrane protrusions called invadopodia, which resemble podosomes. They are primary sites of rapid actin polymerization and major sites of matrix degradation. Invadopodia contain several proteases such as membrane-type 1 matrix metalloproteinase (MT1-MMP) and seprase, which are used for degrading the basement membrane. Myo10 localizes to invadopodia, and Myo10 knockdown in a breast cancer cell line reduces invadopodia formation (Schoumacher et al. 2010).

Both podosomes and invadopodia are cell matrix adhesion sites that connect the cortical actin cytoskeleton within the cell to the ECM. Although many of the same proteins are found in both podosomes and invadopodia including integrin, talin, and paxillin, their structures and dynamics differ. The ability to degrade ECM in order to move through tissue barriers is a hallmark of invasive tumors. At the subcellular level, ECM-degrading activity occurs at the tips of invadopodia where Myo10 accumulates.

17.4.3 Tunneling Nanotubes (TNTs)

In 2004, Ruston and colleagues discovered thin structures connecting single cells over long distances *in vitro* and named them tunneling nanotubes (TNTs) (Appenzeller et al. 2004). TNTs hover above the cell culture substrate and contain a straight, continuous actin rod enclosed in a lipid bilayer. Since then, TNTs have been noted in many different cell types and shown to act as conduits for the intercellular transfer of cellular compounds (Appenzeller et al. 2004; Gurke et al. 2008), transmission of depolarization signals (Wang et al. 2010, 2012; Wittig et al. 2012), spreading of pathogens (Onfelt et al. 2006; Sowinski et al. 2008), and transfer of proteins implicated in disease such as prions, misfolded huntingtin, and pathological Tau protein assemblies (Gousset et al. 2009; Costanzo et al. 2013; Tardivel et al. 2016). In 2013, Myo10 was first reported as a key regulator for TNT formation by interacting with several transmembrane proteins

(Gousset et al. 2013). Thus, it is probable that Myo10 plays a significant role in the induction of TNT and in TNT-mediated biological and pathological functions.

17.4.4 Pseudopods

Pseudopods ("false feet") are large dynamic protrusions found at the front of migrating cells. The term is used broadly to describe actin-rich membrane protrusions without the defined geometry of lamellipodia or filopodia. Thus, the definition of pseudopod varies among cell types. In macrophages, pseudopods are defined as the leading protrusions of phagocytic cups, Myo10 was identified as essential for pseudopod extension during phagocytosis (Cox et al. 2002).

Pseudopods support cancer cell migration and metastasis. Multiple filopodia are induced at the front of pseudopods where they pull on collagen fibrils resulting in a change in the position of both the fibrils and filopodia (Starke et al. 2013). Multiple Myo10-positive filopodia were observed at the front of pseudopods protruding from migrating mouse melanoma cells cultured in 3D collagen matrices. The number of cells with long pseudopods was less in Myo10-kd vs. control cells (Tokuo et al. 2018). These results suggest that Myo10 plays important roles in pseudopod formation, which drives cell migration.

17.5 Expression and Function of Myo10

Myo10 protein expression is observed in all vertebrate tissues (Berg et al. 2000; Yonezawa et al. 2000; Yonezawa et al. 2003), and the functional importance of this motor protein has been found in several different cells and tissues including phagocytic cup formation in leukocytes (Cox et al. 2002), nuclear anchoring and spindle assembly during meiosis in *Xenopus laevis* (Weber et al. 2004), orientation of the mitotic spindle in cultured cells (Toyoshima and Nishida 2007), endothelial cell migration and angiogenesis (Pi et al.

2007), axonal path-finding regulated by netrin (Zhu et al. 2007), migration of cranial neural crest cells in *Xenopus* (Nie et al. 2009; Hwang et al. 2009), sealing zone patterning (McMichael et al. 2010) and differentiation (Tasca et al. 2017) in osteoclasts, barrier formation at tight junctions in polarized epithelial cells (Liu et al. 2012), axon outgrowth in cortical neurons (Raines et al. 2012), cell-to-cell spreading of *Shigella* by membrane protrusions (Bishai et al. 2013), dendritic spine development by VASP transport (Lin et al. 2013), and leukocyte extravasation through cultured endothelial cells (Kroon et al. 2018). Most recently, diminished filopodia formation was detected in isolated macrophages from Myo10KO mice (Horsthemke et al. 2017) and in retinal angiogenesis in the eyes of Myo10KO mice (Heimsath et al. 2017).

17.5.1 Myo10 Functions *In Vivo*

The ability to knockout specific genes in mice has been instrumental in elucidating gene function *in vivo*. The Sanger Mouse Genetics Project generated Myo10KO (*Myo10^{tm2(KOMP)Wtsi}*; *Myo10*^{tm2/tm2}) mice in 2013. After crossing heterozygous *Myo10^{+/tm2}* mice with each other, we obtained *Myo10^{tm2/tm2}* pups at almost the same rate as observed with the Myo10KO mice *Myo10^{tm1d/tm1d}*, *Myo10^{tm1a/tm1a}* and *Myo10^{m1J/m1J}*, in which both full-length and headless Myo10 were deleted (total-KO) (Heimsath et al. 2017). A white spot on the belly was observed with 100% penetrance in *Myo10^{tm2/tm2}* mice, the same rate as in total-KO mice. The number of melanocytes in the white patches of the *Myo10^{tm2/tm2}* mice was significantly reduced vs. dark patches on wild-type mice, evidence that depletion of Myo10 in the melanocyte lineage reduces the number of melanocytes in the white belly spots resulting in a pigmentation defect. *Myo10^{tm2/tm2}* mice also exhibit syndactyly in the form of webbed digits in the forelimbs or hind legs, with a slightly higher rate than that observed in total-KO mice. The International Mouse Phenotyping Consortium (IMPC) reported that *Myo10^{tm2/tm2}*

mice had persistent hyaloid vasculature, fused cornea and lens, corneal opacity, and an abnormal pupil light response. These abnormal phenotypes in eyes are similar to those found in the total-KO mice, which exhibited persistent hyaloid vasculature (Heimsath et al. 2017). Other phenotypes related to the *Myo10^{tm2(KOMP)Wtsi}* allele including fused phalanges are described on the IMPC website (http://www.mousephenotype.org/data/genes/MGI:107716).

These findings suggest that the phenotype of the full-length Myo10 only KO mouse (*Myo10^{tm2/tm2}*) is nearly identical as that of the total KO mouse. This observation is understandable because most tissues express only full-length Myo10, whereas neuronal cells (neural stem cells, neurons, and astrocytes) express both full-length and headless Myo10 (Sousa et al. 2006; Raines et al. 2012). Thus, the difference between the total Myo10 KO mouse and the full-length only Myo10 KO mouse is due to depleted expression of headless Myo10 in neuronal cells. One idea is that headless Myo10 is a negative regulator of full-length Myo10 (Raines et al. 2012), but whether headless Myo10 plays other functions is unknown.

17.5.2 Myo10 in Melanoblast Migration

Studies of naturally occurring mutations that lead to white belly spots in mice have significantly increased our understanding of melanoblast (precursors to melanocytes) migration including the identification of molecules essential for melanoblast migration. To investigate the effects of *Myo10* loss on melanoblast function, we reduced Myo10 expression in the mouse melanoblast cell line Melb-a with short hairpin RNA (shRNA). Melb-a cells retain the character of melanoblasts versus that of mature melanocytes or melanoma cells (Sviderskaya et al. 1995). The number of cells with long pseudopods was significantly lower in Myo10kd vs. control cells cultured on collagen matrices, and the migration rate of Myo10kd cells was slower than control cells (Tokuo et al. 2018). These results are consistent with studies show-

ing that Myo10kd inhibits migration of breast cancer cells (Cao et al. 2014). Together, the studies indicate that long pseudopods play a major role in the migration of melanoblasts and that Myo10 is required for pseudopod formation.

17.6 Myo10 in Cancer

Recently, Myo10 was found to play important roles in a variety of cancers, e.g., increased MYO10 expression correlates with aggressiveness and metastasis of breast cancer (Cao et al. 2014; Arjonen et al. 2014); expression of MYO10 is up-regulated and contributes to lung adenocarcinoma metastasis (Bidkhori et al. 2013); the *MYO10* gene is a target of microRNA-124, which is suppressed in aggressive non-small cell lung cancer (Sun et al. 2015) and also a target of microRNA-340, which impedes the metastasis of breast cancer (Chen et al. 2016); MYO10 expression is higher in prostate cancer than in normal tissue; and MYO10kd reduces the migratory speed and directional persistence of a prostate cancer cell line (Makowska et al. 2015).

17.6.1 Myo10 in a Mouse Melanoma Model

Melanoblast migration in development correlates well with melanoma metastasis, and past migratory behavior in melanoblasts may incline primary melanomas to form remote metastases (Gupta et al. 2005; Uong and Zon 2010; Strizzi et al. 2011). Thus, Myo10 may function in melanoma metastasis as well as melanoblast migration.

To study this, we employed a mouse melanoma induction model consisting of mice with melanocyte-specific expression of activated Braf, a proto-oncogene, combined with silencing of the Pten tumor suppressor gene (Tyr-CreER/BrafCA/PtenKO); all Tyr-CreER/BrafCA/PtenKO mice develop melanoma (Dankort et al. 2009). When Myo10KO mice were crossed with Tyr-CreER/BrafCA/PtenKO mice, tumor formation was delayed, the average tumor volumes were markedly reduced, lymph node metastasis was significantly decreased, and the medial survival time was significantly extended in Tyr-CreER/BrafCA/PtenKO/Myo10KO mice vs. Tyr-CreER/BrafCA/PtenKO/Myo10 wild type mice (Tokuo et al. 2018), evidence that Myo10 is involved in melanoma initiation and development.

17.6.2 Myo10 in Human Melanoma

Using the PROGgeneV2 prognostic biomarker identification tool (Goswami and Nakshatri 2014), we found in studies designed to investigate the role of Myo10 in human melanoma patients that the amount of *MYO10* mRNA was significantly higher in malignant melanoma than in benign nevi and that elevated expression of the *MYO10* gene was associated with inferior survival outcomes (Tokuo et al. 2018). We also investigated MYO10 protein expression in human melanoma and nevi using a tissue microarray and found that MYO10 staining intensity was significantly higher in melanoma lesions than in nevi, consistent with the results showing that *MYO10* mRNA expression is higher in melanoma vs. benign nevi. These results suggest that the Myo10 expression level correlates with melanocytic neoplastic progression in humans and overall survival of melanoma patients.

17.7 Summary and Perspectives

Myo10 has been studied in many types of cells and organs, and regulation of actin-based protrusions is the main physiological function of this interesting motor protein. These findings are now confirmed in Myo10KO mice, which will continue to provide opportunities for in-depth analyses of the biological and pathological functions of Myo10 *in vivo*. For example, the function of headless Myo10 *in vivo* should be investigated by comparing neuronal function in *total Myo10* KO mice vs. *full-length Myo10 only* KO mice to give new insights into motor domain regulations. Also, in particular, human diseases (including

cancer) related to MYO10 should be reconstructed in mice and challenged for the development of new therapies.

References

Almagro S, Durmort C, Chervin-Petinot A, Heyraud S, Dubois M, Lambert O, Maillefaud C, Hewat E, Schaal JP, Huber P, Gulino-Debrac D (2010) The motor protein myosin-X transports VE-cadherin along filopodia to allow the formation of early endothelial cell-cell contacts. Mol Cell Biol 30(7):1703–1717. https://doi.org/10.1128/MCB.01226-09

Appenzeller J, Lin YM, Knoch J, Avouris P (2004) Band-to-band tunneling in carbon nanotube field-effect transistors. Phys Rev Lett 93(19):196805. https://doi.org/10.1103/PhysRevLett.93.196805

Applewhite DA, Barzik M, Kojima S, Svitkina TM, Gertler FB, Borisy GG (2007) Ena/VASP proteins have an anti-capping independent function in filopodia formation. Mol Biol Cell 18(7):2579–2591

Arjonen A, Kaukonen R, Mattila E, Rouhi P, Hognas G, Sihto H, Miller BW, Morton JP, Bucher E, Taimen P, Virtakoivu R, Cao Y, Sansom OJ, Joensuu H, Ivaska J (2014) Mutant p53-associated myosin-X upregulation promotes breast cancer invasion and metastasis. J Clin Invest 124(3):1069–1082. https://doi.org/10.1172/JCI67280

Berg JS, Cheney RE (2002) Myosin-X is an unconventional myosin that undergoes intrafilopodial motility. Nat Cell Biol 4(3):246–250

Berg JS, Derfler BH, Pennisi CM, Corey DP, Cheney RE (2000) Myosin-X, a novel myosin with pleckstrin homology domains, associates with regions of dynamic actin. J Cell Sci 113(Pt 19):3439–3451

Bidkhori G, Narimani Z, Hosseini Ashtiani S, Moeini A, Nowzari-Dalini A, Masoudi-Nejad A (2013) Reconstruction of an integrated genome-scale co-expression network reveals key modules involved in lung adenocarcinoma. PLoS One 8(7):e67552. https://doi.org/10.1371/journal.pone.0067552

Bishai EA, Sidhu GS, Li W, Dhillon J, Bohil AB, Cheney RE, Hartwig JH, Southwick FS (2013) Myosin-X facilitates Shigella-induced membrane protrusions and cell-to-cell spread. Cell Microbiol 15(3):353–367. https://doi.org/10.1111/cmi.12051

Bohil AB, Robertson BW, Cheney RE (2006) Myosin-X is a molecular motor that functions in filopodia formation. Proc Natl Acad Sci U S A 103(33):12411–12416

Cao R, Chen J, Zhang X, Zhai Y, Qing X, Xing W, Zhang L, Malik YS, Yu H, Zhu X (2014) Elevated expression of myosin X in tumours contributes to breast cancer aggressiveness and metastasis. Br J Cancer 111(3):539–550. https://doi.org/10.1038/bjc.2014.298

Caride AJ, Bennett RD, Strehler EE (2010) Kinetic analysis reveals differences in the binding mechanism of calmodulin and calmodulin-like protein to the IQ motifs of myosin-10. Biochemistry 49(37):8105–8116. https://doi.org/10.1021/bi100644q

Chan PC, Hsu RY, Liu CW, Lai CC, Chen HC (2014) Adducin-1 is essential for mitotic spindle assembly through its interaction with myosin-X. J Cell Biol 204(1):19–28. https://doi.org/10.1083/jcb.201306083

Chen ZY, Hasson T, Kelley PM, Schwender BJ, Schwartz MF, Ramakrishnan M, Kimberling WJ, Mooseker MS, Corey DP (1996) Molecular cloning and domain structure of human myosin-VIIa, the gene product defective in usher syndrome 1B. Genomics 36(3):440–448. https://doi.org/10.1006/geno.1996.0489

Chen CP, Sun ZL, Lu X, Wu WX, Guo WL, Lu JJ, Han C, Huang JQ, Fang Y (2016) MiR-340 suppresses cell migration and invasion by targeting MYO10 in breast cancer. Oncol Rep 35(2):709–716. https://doi.org/10.3892/or.2015.4411

Chishti AH, Kim AC, Marfatia SM, Lutchman M, Hanspal M, Jindal H, Liu SC, Low PS, Rouleau GA, Mohandas N, Chasis JA, Conboy JG, Gascard P, Takakuwa Y, Huang SC, Benz EJ Jr, Bretscher A, Fehon RG, Gusella JF, Ramesh V, Solomon F, Marchesi VT, Tsukita S, Tsukita S, Hoover KB et al (1998) The FERM domain: a unique module involved in the linkage of cytoplasmic proteins to the membrane. Trends Biochem Sci 23(8):281–282

Costanzo M, Abounit S, Marzo L, Danckaert A, Chamoun Z, Roux P, Zurzolo C (2013) Transfer of polyglutamine aggregates in neuronal cells occurs in tunneling nanotubes. J Cell Sci 126(Pt 16):3678–3685. https://doi.org/10.1242/jcs.126086

Cox D, Berg JS, Cammer M, Chinegwundoh JO, Dale BM, Cheney RE, Greenberg S (2002) Myosin X is a downstream effector of PI(3)K during phagocytosis. Nat Cell Biol 4(7):469–477

Dankort D, Curley DP, Cartlidge RA, Nelson B, Karnezis AN, Damsky WE Jr, You MJ, DePinho RA, McMahon M, Bosenberg M (2009) Braf(V600E) cooperates with Pten loss to induce metastatic melanoma. Nat Genet 41(5):544–552. https://doi.org/10.1038/ng.356

Divito MM, Cheney RE (2008) Myosins: a superfamily of molecular motors chapter 14 MYOSIN X. In: Proteins and cell regulation, vol 7. Springer, Dordrecht

Frame MC, Patel H, Serrels B, Lietha D, Eck MJ (2010) The FERM domain: organizing the structure and function of FAK. Nat Rev Mol Cell Biol 11(11):802–814. https://doi.org/10.1038/nrm2996

Fukuda M, Mikoshiba K (1996) Structure-function relationships of the mouse Gap1m. Determination of the inositol 1,3,4,5-tetrakisphosphate-binding domain. J Biol Chem 271(31):18838–18842

Goswami CP, Nakshatri H (2014) PROGgeneV2: enhancements on the existing database. BMC Cancer 14:970. https://doi.org/10.1186/1471-2407-14-970

Gousset K, Schiff E, Langevin C, Marijanovic Z, Caputo A, Browman DT, Chenouard N, de Chaumont F, Martino A, Enninga J, Olivo-Marin JC, Mannel D, Zurzolo C (2009) Prions hijack tunnelling nanotubes for intercellular spread. Nat Cell Biol 11(3):328–336. https://doi.org/10.1038/ncb1841

Gousset K, Marzo L, Commere PH, Zurzolo C (2013) Myo10 is a key regulator of TNT formation in neuronal cells. J Cell Sci 126(Pt 19):4424–4435. https://doi.org/10.1242/jcs.129239

Gupta PB, Kuperwasser C, Brunet JP, Ramaswamy S, Kuo WL, Gray JW, Naber SP, Weinberg RA (2005) The melanocyte differentiation program predisposes to metastasis after neoplastic transformation. Nat Genet 37(10):1047–1054. https://doi.org/10.1038/ng1634

Gurke S, Barroso JF, Hodneland E, Bukoreshtliev NV, Schlicker O, Gerdes HH (2008) Tunneling nanotube (TNT)-like structures facilitate a constitutive, actomyosin-dependent exchange of endocytic organelles between normal rat kidney cells. Exp Cell Res 314(20):3669–3683. https://doi.org/10.1016/j.yexcr.2008.08.022

Hammer JA 3rd (1994) The structure and function of unconventional myosins: a review. J Muscle Res Cell Motil 15(1):1–10

Haslam RJ, Koide HB, Hemmings BA (1993) Pleckstrin domain homology. Nature 363(6427):309–310. https://doi.org/10.1038/363309b0

Heimsath EG Jr, Yim YI, Mustapha M, Hammer JA, Cheney RE (2017) Myosin-X knockout is semi-lethal and demonstrates that myosin-X functions in neural tube closure, pigmentation, hyaloid vasculature regression, and filopodia formation. Sci Rep 7(1):17354. https://doi.org/10.1038/s41598-017-17638-x

Hirano Y, Hatano T, Takahashi A, Toriyama M, Inagaki N, Hakoshima T (2011) Structural basis of cargo recognition by the myosin-X MyTH4-FERM domain. EMBO J 30(13):2734–2747. https://doi.org/10.1038/emboj.2011.177

Homma K, Saito J, Ikebe R, Ikebe M (2001) Motor function and regulation of myosin X. J Biol Chem 276(36):34348–34354

Horsthemke M, Bachg AC, Groll K, Moyzio S, Muther B, Hemkemeyer SA, Wedlich-Soldner R, Sixt M, Tacke S, Bahler M, Hanley PJ (2017) Multiple roles of filopodial dynamics in particle capture and phagocytosis and phenotypes of Cdc42 and Myo10 deletion. J Biol Chem 292(17):7258–7273. https://doi.org/10.1074/jbc.M116.766923

Hwang YS, Luo T, Xu Y, Sargent TD (2009) Myosin-X is required for cranial neural crest cell migration in Xenopus laevis. Dev Dyn 238(10):2522–2529

Isakoff SJ, Cardozo T, Andreev J, Li Z, Ferguson KM, Abagyan R, Lemmon MA, Aronheim A, Skolnik EY (1998) Identification and analysis of PH domain-containing targets of phosphatidylinositol 3-kinase using a novel in vivo assay in yeast. EMBO J 17(18):5374–5387. https://doi.org/10.1093/emboj/17.18.5374

Kerber ML, Cheney RE (2011) Myosin-X: a MyTH-FERM myosin at the tips of filopodia. J Cell Sci 124(Pt 22):3733–3741. https://doi.org/10.1242/jcs.023549

Kerber ML, Jacobs DT, Campagnola L, Dunn BD, Yin T, Sousa AD, Quintero OA, Cheney RE (2009) A novel form of motility in filopodia revealed by imaging myosin-X at the single-molecule level. Curr Biol 19(11):967–973

Knight PJ, Thirumurugan K, Xu Y, Wang F, Kalverda AP, Stafford WF 3rd, Sellers JR, Peckham M (2005) The predicted coiled-coil domain of myosin 10 forms a novel elongated domain that lengthens the head. J Biol Chem 280(41):34702–34708

Kroon J, Schaefer A, van Rijssel J, Hoogenboezem M, van Alphen F, Hordijk P, Stroes ESG, Stromblad S, van Rheenen J, van Buul JD (2018) Inflammation-sensitive myosin-X functionally supports leukocyte extravasation by Cdc42-mediated ICAM-1-rich endothelial Filopodia formation. J Immunol 200(5):1790–1801. https://doi.org/10.4049/jimmunol.1700702

Kwon M, Bagonis M, Danuser G, Pellman D (2015) Direct microtubule-binding by Myosin-10 orients centrosomes toward retraction fibers and subcortical actin clouds. Dev Cell 34(3):323–337. https://doi.org/10.1016/j.devcel.2015.06.013

Lin WH, Hurley JT, Raines AN, Cheney RE, Webb DJ (2013) Myosin X and its motorless isoform differentially modulate dendritic spine development by regulating trafficking and retention of vasodilator-stimulated phosphoprotein. J Cell Sci 126(Pt 20):4756–4768. https://doi.org/10.1242/jcs.132969

Liu KC, Jacobs DT, Dunn BD, Fanning AS, Cheney RE (2012) Myosin-X functions in polarized epithelial cells. Mol Biol Cell 23(9):1675–1687. https://doi.org/10.1091/mbc.E11-04-0358

Lu Q, Ye F, Wei Z, Wen Z, Zhang M (2012) Antiparallel coiled-coil-mediated dimerization of myosin X. Proc Natl Acad Sci U S A 109(43):17388–17393. https://doi.org/10.1073/pnas.1208642109

Makowska KA, Hughes RE, White KJ, Wells CM, Peckham M (2015) Specific Myosins control actin organization, cell morphology, and migration in prostate Cancer cells. Cell Rep 13(10):2118–2125. https://doi.org/10.1016/j.celrep.2015.11.012

Mattila PK, Lappalainen P (2008) Filopodia: molecular architecture and cellular functions. Nat Rev Mol Cell Biol 9(6):446–454. https://doi.org/10.1038/nrm2406

Mayer BJ, Ren R, Clark KL, Baltimore D (1993) A putative modular domain present in diverse signaling proteins. Cell 73(4):629–630

McMichael BK, Cheney RE, Lee BS (2010) Myosin X regulates sealing zone patterning in osteoclasts through linkage of podosomes and microtubules. J Biol Chem 285(13):9506–9515. https://doi.org/10.1074/jbc.M109.017269

Nagy S, Ricca BL, Norstrom MF, Courson DS, Brawley CM, Smithback PA, Rock RS (2008) A myosin motor

that selects bundled actin for motility. Proc Natl Acad Sci U S A 105(28):9616–9620

Nie S, Kee Y, Bronner-Fraser M (2009) Myosin-X is critical for migratory ability of Xenopus cranial neural crest cells. Dev Biol 335(1):132–142

Onfelt B, Nedvetzki S, Benninger RK, Purbhoo MA, Sowinski S, Hume AN, Seabra MC, Neil MA, French PM, Davis DM (2006) Structurally distinct membrane nanotubes between human macrophages support long-distance vesicular traffic or surfing of bacteria. J Immunol 177(12):8476–8483

Pi X, Ren R, Kelley R, Zhang C, Moser M, Bohil AB, Divito M, Cheney RE, Patterson C (2007) Sequential roles for myosin-X in BMP6-dependent filopodial extension, migration, and activation of BMP receptors. J Cell Biol 179(7):1569–1582

Plantard L, Arjonen A, Lock JG, Nurani G, Ivaska J, Stromblad S (2010) PtdIns(3,4,5)P(3) is a regulator of myosin-X localization and filopodia formation. J Cell Sci 123(Pt 20):3525–3534. https://doi.org/10.1242/jcs.069609

Raines AN, Nagdas S, Kerber ML, Cheney RE (2012) Headless Myo10 is a negative regulator of full-length Myo10 and inhibits axon outgrowth in cortical neurons. J Biol Chem 287(30):24873–24883. https://doi.org/10.1074/jbc.M112.369173

Rameh LE, Arvidsson A, Carraway KL 3rd, Couvillon AD, Rathbun G, Crompton A, VanRenterghem B, Czech MP, Ravichandran KS, Burakoff SJ, Wang DS, Chen CS, Cantley LC (1997) A comparative analysis of the phosphoinositide binding specificity of pleckstrin homology domains. J Biol Chem 272(35):22059–22066

Rogers MS, Strehler EE (2001) The tumor-sensitive calmodulin-like protein is a specific light chain of human unconventional myosin X. J Biol Chem 276(15):12182–12189

Ropars V, Yang Z, Isabet T, Blanc F, Zhou K, Lin T, Liu X, Hissier P, Samazan F, Amigues B, Yang ED, Park H, Pylypenko O, Cecchini M, Sindelar CV, Sweeney HL, Houdusse A (2016) The myosin X motor is optimized for movement on actin bundles. Nat Commun 7:12456. https://doi.org/10.1038/ncomms12456

Salim K, Bottomley MJ, Querfurth E, Zvelebil MJ, Gout I, Scaife R, Margolis RL, Gigg R, Smith CI, Driscoll PC, Waterfield MD, Panayotou G (1996) Distinct specificity in the recognition of phosphoinositides by the pleckstrin homology domains of dynamin and Bruton's tyrosine kinase. EMBO J 15(22):6241–6250

Schoumacher M, Goldman RD, Louvard D, Vignjevic DM (2010) Actin, microtubules, and vimentin intermediate filaments cooperate for elongation of invadopodia. J Cell Biol 189(3):541–556. https://doi.org/10.1083/jcb.200909113

Shaw G (1993) Identification of novel pleckstrin homology (PH) domains provides a hypothesis for PH domain function. Biochem Biophys Res Commun 195(2):1145–1151. https://doi.org/10.1006/bbrc.1993.2164

Solc CK, Derfler BH, Duyk GM, Corey DP (1994) Molecular cloning of myosins from the bullfrog saccular macula: a candidate for the hair cell adaptation motor. Aud Neurosci 1:63–75

Sousa AD, Berg JS, Robertson BW, Meeker RB, Cheney RE (2006) Myo10 in brain: developmental regulation, identification of a headless isoform and dynamics in neurons. J Cell Sci 119(Pt 1):184–194

Sowinski S, Jolly C, Berninghausen O, Purbhoo MA, Chauveau A, Kohler K, Oddos S, Eissmann P, Brodsky FM, Hopkins C, Onfelt B, Sattentau Q, Davis DM (2008) Membrane nanotubes physically connect T cells over long distances presenting a novel route for HIV-1 transmission. Nat Cell Biol 10(2):211–219. https://doi.org/10.1038/ncb1682

Starke J, Maaser K, Wehrle-Haller B, Friedl P (2013) Mechanotransduction of mesenchymal melanoma cell invasion into 3D collagen lattices: filopod-mediated extension-relaxation cycles and force anisotropy. Exp Cell Res 319(16):2424–2433. https://doi.org/10.1016/j.yexcr.2013.04.003

Strizzi L, Hardy KM, Kirsammer GT, Gerami P, Hendrix MJ (2011) Embryonic signaling in melanoma: potential for diagnosis and therapy. Lab Investig 91(6):819–824. https://doi.org/10.1038/labinvest.2011.63

Sun Y, Ai X, Shen S, Lu S (2015) NF-kappaB-mediated miR-124 suppresses metastasis of non-small-cell lung cancer by targeting MYO10. Oncotarget 6(10):8244–8254. https://doi.org/10.18632/oncotarget.3135

Sviderskaya EV, Wakeling WF, Bennett DC (1995) A cloned, immortal line of murine melanoblasts inducible to differentiate to melanocytes. Development 121(5):1547–1557

Tardivel M, Begard S, Bousset L, Dujardin S, Coens A, Melki R, Buee L, Colin M (2016) Tunneling nanotube (TNT)-mediated neuron-to neuron transfer of pathological Tau protein assemblies. Acta Neuropathol Commun 4(1):117. https://doi.org/10.1186/s40478-016-0386-4

Tasca A, Astleford K, Lederman A, Jensen ED, Lee BS, Gopalakrishnan R, Mansky KC (2017) Regulation of osteoclast differentiation by myosin X. Sci Rep 7(1):7603. https://doi.org/10.1038/s41598-017-07855-9

Tokuo H, Ikebe M (2004) Myosin X transports Mena/VASP to the tip of filopodia. Biochem Biophys Res Commun 319(1):214–220

Tokuo H, Mabuchi K, Ikebe M (2007) The motor activity of myosin-X promotes actin fiber convergence at the cell periphery to initiate filopodia formation. J Cell Biol 179(2):229–238. https://doi.org/10.1083/jcb.200703178

Tokuo H, Bhawan J, Coluccio LM (2018) Myosin X is required for efficient melanoblast migration and melanoma initiation and metastasis. Sci Rep 8(1):10449. https://doi.org/10.1038/s41598-018-28717-y

Toyoshima F, Nishida E (2007) Integrin-mediated adhesion orients the spindle parallel to the substratum in an EB1- and myosin X-dependent manner. EMBO J 26(6):1487–1498

Umeki N, Jung HS, Sakai T, Sato O, Ikebe R, Ikebe M (2011) Phospholipid-dependent regulation of the motor activity of myosin X. Nat Struct Mol Biol 18(7):783–788. https://doi.org/10.1038/nsmb.2065

Uong A, Zon LI (2010) Melanocytes in development and cancer. J Cell Physiol 222(1):38–41. https://doi.org/10.1002/jcp.21935

Wang A, Liang Y, Fridell RA, Probst FJ, Wilcox ER, Touchman JW, Morton CC, Morell RJ, Noben-Trauth K, Camper SA, Friedman TB (1998) Association of unconventional myosin MYO15 mutations with human nonsyndromic deafness DFNB3. Science 280(5368):1447–1451

Wang X, Veruki ML, Bukoreshtliev NV, Hartveit E, Gerdes HH (2010) Animal cells connected by nanotubes can be electrically coupled through interposed gap-junction channels. Proc Natl Acad Sci U S A 107(40):17194–17199. https://doi.org/10.1073/pnas.1006785107

Wang X, Bukoreshtliev NV, Gerdes HH (2012) Developing neurons form transient nanotubes facilitating electrical coupling and calcium signaling with distant astrocytes. PLoS One 7(10):e47429. https://doi.org/10.1371/journal.pone.0047429

Watanabe TM, Tokuo H, Gonda K, Higuchi H, Ikebe M (2010) Myosin-X induces filopodia by multiple elongation mechanism. J Biol Chem 285(25):19605–19614. https://doi.org/10.1074/jbc.M109.093864

Weber KL, Sokac AM, Berg JS, Cheney RE, Bement WM (2004) A microtubule-binding myosin required for nuclear anchoring and spindle assembly. Nature 431(7006):325–329

Wei Z, Yan J, Lu Q, Pan L, Zhang M (2011) Cargo recognition mechanism of myosin X revealed by the structure of its tail MyTH4-FERM tandem in complex with the DCC P3 domain. Proc Natl Acad Sci U S A 108(9):3572–3577. https://doi.org/10.1073/pnas.1016567108

Wittig D, Wang X, Walter C, Gerdes HH, Funk RH, Roehlecke C (2012) Multi-level communication of human retinal pigment epithelial cells via tunneling nanotubes. PLoS One 7(3):e33195. https://doi.org/10.1371/journal.pone.0033195

Wu L, Pan L, Wei Z, Zhang M (2011) Structure of MyTH4-FERM domains in myosin VIIa tail bound to cargo. Science 331(6018):757–760. https://doi.org/10.1126/science.1198848

Yonezawa S, Kimura A, Koshiba S, Masaki S, Ono T, Hanai A, Sonta S, Kageyama T, Takahashi T, Moriyama A (2000) Mouse myosin X: molecular architecture and tissue expression as revealed by northern blot and in situ hybridization analyses. Biochem Biophys Res Commun 271(2):526–533

Yonezawa S, Yoshizaki N, Sano M, Hanai A, Masaki S, Takizawa T, Kageyama T, Moriyama A (2003) Possible involvement of myosin-X in intercellular adhesion: importance of serial pleckstrin homology regions for intracellular localization. Develop Growth Differ 45(2):175–185

Yu H, Wang N, Ju X, Yang Y, Sun D, Lai M, Cui L, Sheikh MA, Zhang J, Wang X, Zhu X (2012) PtdIns (3,4,5) P3 recruitment of Myo10 is essential for axon development. PLoS One 7(5):e36988. https://doi.org/10.1371/journal.pone.0036988

Zhang H, Berg JS, Li Z, Wang Y, Lang P, Sousa AD, Bhaskar A, Cheney RE, Stromblad S (2004) Myosin-X provides a motor-based link between integrins and the cytoskeleton. Nat Cell Biol 6(6):523–531. https://doi.org/10.1038/ncb1136

Zhu XJ, Wang CZ, Dai PG, Xie Y, Song NN, Liu Y, Du QS, Mei L, Ding YQ, Xiong WC (2007) Myosin X regulates netrin receptors and functions in axonal path-finding. Nat Cell Biol 9(2):184–192